The Journal of Immunology

TCR Signal Transduction in Antigen-Specific Memory CD8 T Cells

Ellen N. Kersh, Susan M. Kaech, Thandi M. Onami, Miriana Moran, E. John Wherry, M. Carrie Miceli and Rafi Ahmed

J Immunol 2003; 170:5455-5463; ;
doi: 10.4049/jimmunol.170.11.5455
http://www.jimmunol.org/content/170/11/5455

The Journal of Immunology is published twice each month by
The American Association of Immunologists, Inc.,
1451 Rockville Pike, Suite 650, Rockville, MD 20852

Print ISSN: 0022-1767 Online ISSN: 1550-6606.

TCR Signal Transduction in Antigen-Specific Memory CD8 T Cells[1]

Ellen N. Kersh,* Susan M. Kaech,* Thandi M. Onami,* Miriana Moran,† E. John Wherry,* M. Carrie Miceli,† and Rafi Ahmed[2]*

Memory T cells are more responsive to Ag than naive cells. To determine whether memory T cells also have more efficient TCR signaling, we compared naive, effector, and memory CD8 T cells of the same antigenic specificity. Surprisingly, initial CD3 signaling events are indistinguishable. However, memory T cells have more extensive lipid rafts with higher phosphoprotein content before TCR engagement. Upon activation in vivo, they more efficiently induce phosphorylation of-LAT (linker for activation of T cells), ERK (extracellular signal-regulated kinase), JNK (c-Jun N-terminal kinase), and p38. Thus, memory CD8 T cells do not increase their TCR sensitivity, but are better poised to augment downstream signals. We propose that this regulatory mechanism might increase signal transduction in memory T cells, while limiting TCR cross-reactivity and autoimmunity. ***The Journal of Immunology*****, 2003, 170: 5455–5463.**

Memory T cells are a differentiated cell type that is functionally more responsive than naive T cells (1–3). One hypothesis is that memory T cells have increased TCR signal transduction, increasing their responsiveness to Ag. In this study, we examine proximal TCR tyrosine phosphorylation events and partitioning of phosphoproteins into lipid rafts in memory CD8 T cells. We activate naive and memory CD8 T cells of the same TCR specificity with Ag and then quantitatively compare the ensuing induction of TCR signaling.

A definitive analysis of signaling intermediates in memory T cells has previously been hampered by the difficulty to obtain enough memory T cells with known activation history. TCR signal transduction has therefore mostly been studied in immortalized T cell lines with unphysiological activation status. Alternatively, freshly isolated T cells have been isolated based on cell surface markers. However, memory cell surface phenotype can be acquired during Ag-independent homeostatic proliferation (4). The activation history of individual cells therefore cannot be ascertained in cell preparations solely based on surface molecules. To obtain memory cells with precisely known activation history, we use TCR transgenic mice reactive against an epitope derived from lymphocytic choriomeningitis virus (LCMV)[3] (5). Infection with LCMV leads to efficient acute activation of transgenic CD8 T cells. Memory CD8 T cells then persist for the lifetime of the animal, and this is independent of the presence of Ag (6, 7).

The TCR complex consists of the $\alpha\beta$ TCR and the CD3 ζ-, ϵ-, γ-, and δ-chains. Upon TCR engagement, *src* kinases $p56^{lck}$ and $p56^{fyn}$ phosphorylate tyrosines in immunoreceptor tyrosine-based activation motifs in the CD3 chains (8, 9). In additon, CD3ϵ undergoes a conformational change and interacts with signaling molecules (10). ZAP-70 kinase binds to the phosphorylated CD3 complex, most notably to CD3ζ, and then is also phosphorylated and activated by $p56^{lck}$. This leads to abundant phosphorylation of downstream signaling proteins. One critical substrate is the linker protein LAT (linker for activation of T cells) (11, 12). Phospho-LAT subsequently activates calcium mobilization, and the Ras/mitogen-activated protein (MAP) kinase signaling pathway.

The plasma membrane is composed of discrete microdomains in which membrane molecules are differentially partitioned (13). These microdomains, also called lipid rafts, are believed to be specialized compartments for signaling complexes during T cell activation (14, 15). LAT is located in lipid rafts, and its localization is required for its phosphorylation.

It is not clear whether TCR signaling is regulated differently in naive, recently activated, and memory CD8 T cells. Resting memory CD4 cells have unique, unidentified phosphoproteins, potentially prewiring them for efficient activation (16, 17). Upon CD3 cross-linking, fewer phosphoproteins, including ZAP-70, are induced, and fewer subsequent steps are involved for MAP kinase activation (18). Very little information is available for memory CD8 T cells, except that more $p56^{lck}$ is localized with the CD8 coreceptor (19), and that the level of $p56^{lck}$ can be higher (20, 21). In activated T cells, the TCR itself is more accessible to binding of MHC dimers, presumably because the TCR is redistributed into lipid rafts (22). Furthermore, the amount of lipid rafts is increased in activated human PBLs (23). However, a definitive analysis has not been undertaken as to how these changes affect signaling intermediates in memory CD8 T cells.

In this study, we examine proximal steps of TCR signal transduction in naive and Ag-experienced CD8 T cells. We compare naive and memory T cells, but we also include effector cells from

*Department of Microbiology and Immunology, Emory Vaccine Center and Emory University School of Medicine, Atlanta, GA 30322; and †Department of Microbiology, Immunology and Molecular Genetics, University of California School of Medicine, Los Angeles, CA 90095

Received for publication January 10, 2003. Accepted for publication March 27, 2003.

The costs of publication of this article were defrayed in part by the payment of page charges. This article must therefore be hereby marked *advertisement* in accordance with 18 U.S.C. Section 1734 solely to indicate this fact.

[1] E.N.K. and S.M.K. were supported by Fellowships DR1604 and DR1570 of the Damon Runyon-Walter Winchell Foundation, respectively. T.M.O. was supported by National Institutes of Health Research Supplement for Underrepresented Minorities Fellowship. M.M. was supported by a fellowship from the Jonsson Comprehensive Cancer Center. E.J.W. was supported by a fellowship from the Cancer Research Institute. This work was supported in part by National Institutes of Health 2ROICA65979 awarded to M.C.M. and National Institutes of Health R37AI30048 to R.A.

[2] Address correspondence and reprint requests to Dr. Rafi Ahmed, Rollins Research Building, Room G211, 1510 Clifton Road, Atlanta, GA 30322. E-mail address: ra@microbio.emory.edu

[3] Abbreviations used in this paper: LCMV, lymphocytic choriomeningitis virus; aGM1, asialo-GM1; CD62L, CD62 ligand; LAT, linker for activation of T cells; MAP, mitogen-activated protein; MKK, MAP kinase kinase; T_{CM}, central memory; T_{EM}, effector memory.

0022-1767/03/$02.00

the peak of the immune response to understand the stability of biochemical changes during the course of an immune response. We dissect the sensitivity of CD3 and ZAP-70 phosphorylation before and after peptide restimulation, as well as after stimulation with suboptimal, altered ligands of this TCR. We then examine LAT localization and phosphorylation, as well as lipid raft size and phosphotyrosine protein content. Finally, we compare active components of the MAP kinase signaling pathway immediately after T cell activation in vivo. Our results reveal that initial TCR signaling events are similar in naive and memory T cells. However, memory T cells have more extensive lipid raft signaling compartments with higher phosphoprotein content, and more efficiently activate the MAP kinase pathway. We propose that this might be a novel regulatory mechanism that preserves the reactivity of the TCR, but increases effectiveness of signal transduction in memory CD8 T cells.

Materials and Methods

Mice and virus infections

P14 transgenic mice (5) were obtained from The Jackson Laboratory (Bar Harbor, ME) and backcrossed to C57BL/6 for 10 generations. Female B6 mice, age 6–8 wk, were purchased from National Cancer Institute, and TCR C$\alpha^{-/-}$ mice (24) from The Jackson Laboratory. Chimeric mice were generated by transfer of 10^6 P14, Thy-1.1$^+$ splenocytes into C57BL/6 mice, followed by infection with 2×10^5 PFU LCMV Armstrong i.p. (25, 26). All mice were maintained according to Emory University's Institutional Review Board.

T cell purification

T cells were strictly kept at 4°C. Splenocytes were incubated with anti-Thy-1.1 FITC (His51; BD PharMingen, San Diego, CA) at 2×10^7/ml in RPMI with 1% FCS for 30 min. After washing, cells were incubated with anti-FITC magnetic beads (Miltenyi Biotec, Auburn, CA) and separated, according to the manufacturer's instructions. Purified cells were analyzed by FACS before each experiment using D^{b}gp33 tetramers and anti-CD8 and anti-CD4. Samples were then adjusted to contain the same number of Ag-specific and other T cells (~60 and 10%, respectively; the remaining 30% cells were non-T cells, mostly B cells). To separate CD62 ligand^{high} (CD62L^{high}) memory cells, anti-CD62L beads (Miltenyi Biotec) were used.

Peptides

Peptide sequences were gp33 (WT), KAVYNFATM; A4Y, KAVAN FATM; A6F, KAVYNAATM; V4Y, KAVVNFATM; S4Y, KAVSN FATM; G4Y, KAVGNFATM; control peptide AV derived from adenovirus, SGPSNTPPEI (27).

T cell stimulation, lysis, immunoprecipitation, and SDS-PAGE

A total of 5–10 $\times$ 10^6 purified Ag-specific T cells was mixed with 10^7 splenocytes from TCR C$\alpha^{-/-}$ mice prepulsed with peptide. Alternatively, we used 4×10^6 freshly isolated macrophages as APCs from peritoneal exudates after thioglycolate treatment of C57BL/6 mice (19) with similar results. Cells were activated in RPMI medium at 37°C for 10 min, unless otherwise indicated. Cells were lysed for 30 min in buffer containing 1% Triton X-100, 20 mM Tris, pH 7.3, 150 mM NaCl, 2 mM EDTA, 10 mM NaF, 400 μM Na_3VO_4, 1 mM PMSF, 2 μg/ml aprotinin, 5 μg/ml leupeptin, and 0.7 μg/ml pepstatin A. Insoluble material was pelleted, and the supernatant was utilized for immunoprecipitation using 5 μg of anti-CD3ϵ (clone 500.A2; BD PharMingen) or 10 μl rabbit anti-ZAP-70 (Santa Cruz Biotechnology, Santa Cruz, CA) and 50 μl of 50% protein A-Sepharose. Proteins were solubilized in reducing Laemmli sample buffer and separated on 12% SDS-PAGE, followed by transfer to nitrocellulose. Separated CD62L$^{high/low}$ memory cells were stimulated in vitro with splenocytes from C57BL/6 mice and 1 μM gp33 peptide for 30 min.

Immunoblotting

Immunoblotting was performed in PBS containing 4% BSA and 0.1% Tween 20. Wash buffer contained PBS and 0.1% Tween 20. For antiphosphotyrosine blotting, we used 4G10 biotin (1 μg/ml) and streptavidin HRP (Southern Biotechnology Associates, Birmingham, AL; 1/55,000). Visualization of proteins was done with SuperSignal (Pierce, Rockford, IL). Densitometry was performed using National Institutes of Health Image software. Dilutions for blotting with rabbit sera were: anti-CD3ζ 777 (28), 1/500; anti-ZAP-70 (Santa Cruz Biotechnology), 1/200; anti-LAT (12), 1/500; followed by donkey anti-rabbit HRP (Jackson ImmunoResearch Laboratories, West Grove, PA) at 1/5000.

Raft fractionation

Raft fractionation was essentially as described previously (29). Cells were incubated in cold buffer A (25 mM Tris-HCl, 150 mM NaCl, 5 mM EDTA, leupeptin and aprotinin at 1 μg/ml, 1 mM PMSF, 1 mM Na_3VO_4) and disrupted by sonication. After centrifugation at 800 $\times$ *g* for 10 min at 4°C, supernatants were incubated in 1% Brij 58. Lysates were mixed with 80% sucrose in buffer A, and overlayed with 2 vol of 30% sucrose and 1 vol of 5% sucrose. Sucrose gradient centrifugation was performed at 200,000 $\times$ *g* for 16 h. Twelve gradient fractions were harvested from the top and analyzed by anti-p56^{lck} immunoblotting. Lipid rafts were in fractions 1–4; soluble proteins in fractions 8–11. These fractions were pooled and concentrated (30). In brief, 150 μl protein sample was incubated with 600 μl methanol and 150 μl chloroform, followed by 450 μl H_2O. The aqueous phase was discarded, and proteins from the chloroform phase were precipitated using 450 μl methanol. Proteins were pelleted, dried, and resuspended in Laemmli sample buffer.

Intracellular cytokine assays

IFN-γ and TNF-α intracellular staining was performed as described (31).

FACS and FACS sorting

FACS sorting was perfomed using anti-CD8α and anti-Thy-1.1. FACS analysis was done with D^{b}gp33 tetramers (31) or with anti-CD8, anti-CD4, and anti-Thy-1.1 (clones 53-6.7, RM4-5, His 51; BD PharMingen), with rabbit anti-aGM1 (Wako Chemicals, Richmond, VA), or with cholera toxin β for GM1 (Sigma-Aldrich, St. Louis, MO). For intracellular analysis of p56^{lck} and p56^{fyn}, Abs 3A5 and goat anti-*fyn* (Santa Cruz Biotechnology) were directly coupled to FITC using a labeling kit from Calbiochem (La Jolla, CA). Isotype control Abs were anti-IgG2b FITC (BD PharMingen) and polyclonal goat FITC serum (Santa Cruz Biotechnology).

In vivo activation of P14 cells

Mice were i.v. injected with 100 μg gp33. After 15 min, mice were sacrificed, and splenocytes were immediately fixed in fresh 2% paraformaldehyde in PBS and permeabilized in 10$\times$ PermWash solution (BD PharMingen). The following Abs were used for FACS: phospho-ERK (extracellular signal-regulated kinase)-1/2 (p44/42, TEY sequence), phospho-LAT (Y191), phospho-p38 (T180/Y182), and phospho-MKK4 (MAP kinase kinases) (T261) (all from Cell Signaling Technology, Beverly, MA); active c-Jun N-terminal kinase (JNK) (TPY region; Promega, Madison, WI); phospho-c-Jun clone KM-1 (Santa Cruz Biotechnology); goat anti-mouse IgG1 FITC (Southern Biotechnology Associates); goat anti-rabbit FITC (Caltag Laboratories, Burlingame, CA); rabbit serum (Santa Cruz Biotechnology); and anti-CD16/32 for FcγR blockade (BD PharMingen).

Results

Purification of Ag-specific P14 cells

Memory CD8 T cells are functionally more responsive to Ag than naive CD8 cells (1–3). They more readily produce cytokines such as IFN-γ and TNF-α (1–3) and acquire cytotoxicity more rapidly after re-exposure to Ag. In this study, we examined changes in the sensitivity of TCR signal transduction that might contribute to increased functional responsiveness in memory CD8 T cells.

We wished to examine memory T cells with known activation history. We therefore used TCR transgenic cells. CD8 T cells from P14 mice are specific for an epitope from the glycoprotein of LCMV, peptide gp33–41 (hereafter referred to as gp33), in the context of H2-D^b (5). When P14 mice are directly infected with LCMV, only a fraction of transgenic cells becomes activated because of high precursor frequency (25). Hence, we adoptively transferred 2×10^5 naive P14, Thy-1.1$^+$ cells into C57BL/6 recipients (Thy-1.2$^+$) before infection (Fig. 1*A*). Effector splenocytes were harvested 7 days after infection, when 31% of splenocytes were D^{b}gp33 specific (Fig. 1*B*). These cells exhibited maximal effector functions, e.g., displayed ex vivo killing (data not

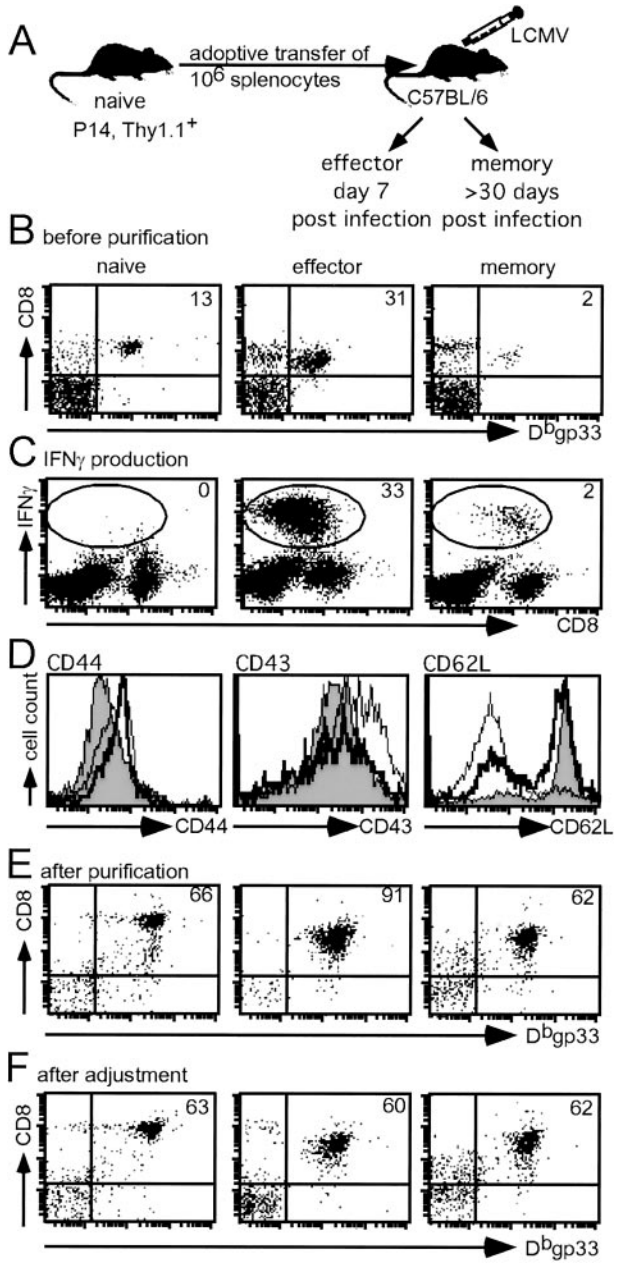

FIGURE 1. Generation and purification of Ag-specific naive, effector, and memory CD8 T cells. *A*, Naive Ag-specific CD8 T cells were obtained from Thy-1.1$^+$ P14 TCR transgenic mice. A total of 1×10^6 splenocytes from P14 mice (containing $\sim 2 \times 10^5$ P14 cells) was transferred into C57BL/6 recipients, followed by infection with LCMV. Effector cells were harvested on day 7 after infection, and memory cells at least 30 days after infection. *B*, Splenocytes were stained with anti-CD8 Ab and D^{b}gp33 tetramer specific for the P14 TCR, followed by FACS analysis. A total of 13, 31, and 2% of splenocytes was Ag specific in naive, effector, and memory samples, respectively. *C*, Naive P14 cells do not produce IFN-γ, while all the effector or memory cells do. Intracellular IFN-γ production was measured by FACS after 5 h of culture with gp33. *D*, P14 cells (D^{b}gp33 tetramer$^+$) were stained with Abs to CD44, CD43, and CD62L (naive, gray filled; effector, thin; memory, bold line). *E*, Purification of Thy-1.1$^+$ P14 cells. Splenocytes were incubated with anti-Thy-1.1 FITC Ab, followed by anti-FITC magnetic beads separation. Greater than 60% of cells are CD8$^+$ and specific for the D^b/gp33 epitope in all preparations. *F*, Samples were adjusted with C57BL/6 splenocytes to contain the same number of P14 cells (60%) and total T cells (data not shown). Cells were stained with anti-CD8 and D^{b}gp33 tetramer, and analyzed by FACS.

shown). Alternatively, memory P14 splenocytes were obtained at least 30 days after infection, when 2% were Ag specific, and Ag has been cleared (6). To examine whether P14 cells had undergone functional maturation, we analyzed their ability to produce IFN-γ after stimulation with peptide gp33 in vitro. Naive P14 splenocytes produced little intracellular IFN-γ, but effector and memory cells readily made IFN-γ at the expected frequency (Fig. 1*C*), also demonstrating that P14 memory cells are indeed more responsive to Ag than naive cells. A set of surface markers including CD44 and CD43 further demonstrated that cells were of naive, effector, or memory phenotype (Fig. 1*D*). All memory P14 cells were homogeneously CD44^{high}. We also analyzed CD62L expression, a marker that distinguishes central memory (T_{CM}, CD62L^{high}) cells and effector memory (T_{EM}) cells (CD62L^{low}) (32). On average, 80% of P14 cells were central memory cells and 20% were effector memory cells.

We next developed a rapid purification scheme to routinely generate 10^7 memory P14 cells. We made use of the Thy-1.1 marker, using anti-Thy-1.1 FITC Ab, followed by anti-FITC magnetic bead cell separation. Cells were strictly kept at 4°C to prevent activation. This yielded a purity of 60–90% P14 cells (Fig. 1*E*), and on average 6×10^6, 13×10^6, and 0.8×10^6 P14 cells per mouse for naive, effector, and memory, respectively. We adjusted samples to contain the same number of P14 cells, as well as of total T cells (CD4$^+$ and CD8$^+$) by adding C57BL/6 splenocytes. As a result, cell samples contained between 60 and 63% P14 cells (Fig. 1*F*) and 70% total T cells (data not shown). It should be noted that effector cells are larger in size than naive and memory cells. Thus, we did not compare equal amounts of protein, but rather one cell to the other. Key experiments were also performed after purification with anti-CD8 to rule out that anti-Thy-1.1 treatment altered activation status, as D^{b}gp33 tetramer did (data not shown).

Equivalent CD3 complex phosphorylation in naive, effector, and memory cells

To assess the signal transduction ability of the TCR, we examined CD3ζ phosphorylation. We specifically activated P14 cells with gp33 peptide-pulsed APCs from TCR C$\alpha^{-/-}$ mice (24) as a source of natural APCs. T cells were stimulated for 10 min, and the TCR complex was precipitated with an Ab to CD3ε (Fig. 2*A*). Surprisingly, we observed no major differences in phosphorylation patterns. P21, the constitutively phosphorylated form of CD3ζ, was phosphorylated to a similar extent in naive, effector, and memory T cells. Upon activation, several phosphoproteins were induced. Most notably, CD3ζ became fully phosphorylated, leading to the appearance of a phosphospecies of 23 kDa (28). The p23:p21 ratio, a measure of efficient CD3ζ phosphorylation, was consistently similar for naive and memory cells (0.31 and 0.36, respectively, in Fig. 2*A*). Although p23/p21 was slightly higher for effector cells in this experiment (0.69, Fig. 2*A*), this was not consistently observed across experiments. An equivalent amount of CD3ζ protein was precipitated in all cells, as immunoblotting with anti-CD3ζ revealed (Fig. 2*A*). Inducible phosphoproteins of 40–50 kDa could also be visualized; the identity of these proteins is unknown. In addition, a phosphoprotein of 70 kDa was induced and identified as ZAP-70, as it comigrated with anti-ZAP-70 immunoprecipitations (data not shown). The phosphorylation of ZAP-70 was surprising, because it is reduced in CD4 memory T cells after CD3 cross-linking (17). Thus, ZAP-70 can be activated in memory CD8 T cells. In summary, we noticed no significant differences in the phosphorylation of the CD3 complex and associated proteins in memory CD8 T cells compared with naive cells.

We next examined the sensitivity to different doses of Ag. Cells were activated with APCs pulsed with increasing doses of peptide

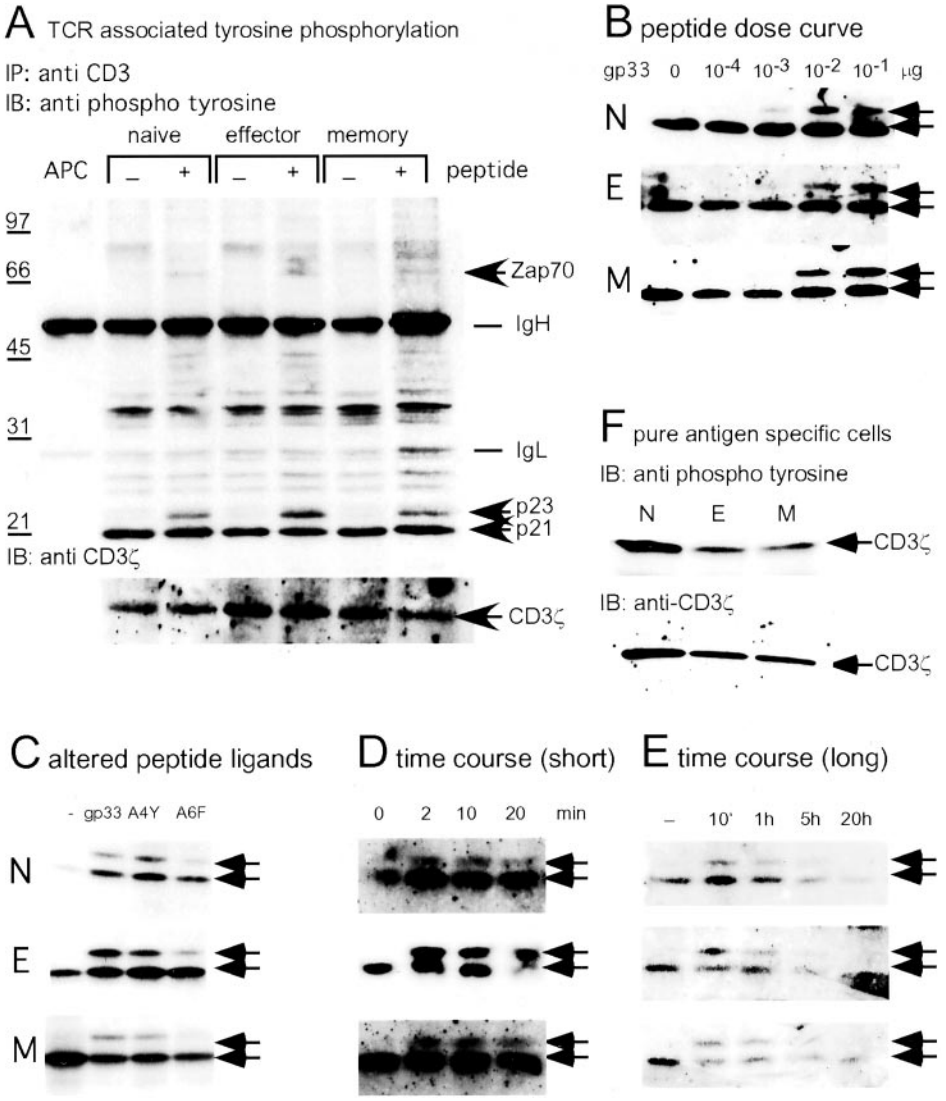

FIGURE 2. Early TCR complex tyrosine phosphorylation events are indistinguishable in naive, effector, and memory P14 cells. *A*, Analysis of CD3ε-associated proteins. A total of 6×10^6 purified P14 cells was stimulated for 10 min with APCs prepulsed with 1 μg gp33. After lysis, the TCR complex was immunoprecipitated (IP) with anti-CD3ε. Proteins were separated by 12% SDS-PAGE and analyzed by antiphosphotyrosine immunoblotting (IB). CD3ζ (p21 and p23) and ZAP-70 were phosphorylated to a similar degree in each cell type. Molecular masses (in kDa) are indicated, as is the size of Ig (IgH and IgL). The nitrocellulose filter was stripped and reprobed with anti-CD3ζ. The experiment is representative of six independent experiments. *B–E*, A total of 4×10^6 purified P14 cells was stimulated with increasing gp33 concentrations (*B*), with 1 μg gp33 or altered peptides A4Y and A6F (*C*), or for various times with gp33 (*D* and *E*). Samples were processed and analyzed as in *A*. Arrows indicate p21 and p23 of CD3ζ. The sensitivity and kinetics of CD3ζ phosphorylation were similar in naive, effector, and memory T cells in five independent experiments for *B*, three for *C*, two for *D*, and three for *E*. *F*, TCR complex phosphorylation in unstimulated, sorted P14 cells. Sorted cells (>97% pure) were directly analyzed for phosphotyrosine or CD3ζ by immunoblotting. The amount of phospho-CD3ζ (p21) and CD3ζ protein was similar in effector and memory T cells, and was higher in naive T cells. Three independent experiments were performed.

gp33 and analyzed as above. In a total of five experiments, we did not find a significant difference among naive, effector, and memory CD8 T cells in their ability to phosphorylate CD3ζ (Fig. 2*B*). In all cell types, fully phosphorylated CD3ζ, p23, was maximally induced with 0.1 μg gp33, and was lower at lower doses. There were slight experimental variations, but the dose curves were consistently similar, and none of the cell types was more sensitive. Phospho-ZAP-70 was also similarly induced (data not shown). Thus, the increased sensitivity of memory and effector CD8 T cells to Ag stimulation is not due to increased signal initiation by the TCR complex itself in response to equivalent Ag stimulation.

The TCR has the ability to respond to a range of ligands, and is not simply an on/off switch receptor (33). It is possible that suboptimal ligands of the P14 TCR stimulate memory P14 cells more effectively. This would indicate that the TCR complex itself is more responsive on memory cells. Alternatively, if the TCR reacts equally to suboptimal ligands, differences in cell responsiveness are likely to be due to other factors such as distal signaling or transcriptional control of effector functions. We therefore stimulated cells with altered peptide ligands of P14. We used five peptides with 1 aa substitution in the gp33–41 sequence (peptides A4Y, A6F, V4Y, S4Y, G4Y), previously defined as partial agonists in naive P14 cells (27). Two peptides, A4Y and A6F, induced intracellular TNF-α after in vitro stimulation in naive, effector, and memory P14 cells. Ligand A4Y was more potent than A6F in naive, effector, and memory cells alike (data not shown). The cells also demonstrated similar sensitivity to increasing doses of A4Y and A6F (data not shown). Most importantly, memory cells did not show responses to more of the altered peptides, and behaved similarly as naive cells (data not shown). Thus, the TCR on naive and memory cells interacts with this panel of ligands equivalently. To further confirm equivalent signal transduction, we also directly examined early TCR complex phosphorylation. The ratio of p23:p21 correlates with functional properties of altered ligands (28). Wt, A4Y, and A6F induced CD3ζ phosphorylation (Fig. 2*C*). The p23:p21 ratios were: 0.62, 0.51, and 0.36 for A4Y for naive, effector, and memory, respectively; 0.38, 0.27, and 0.24 for A6F. Thus, memory cells did not have higher p23:p21 ratios as would have been expected for more efficient signaling. We could not induce CD3ζ phosphorylation with peptides V4Y, S4Y, and G4Y, and control peptide AV (data not shown), as these peptides also did not stimulate TNF-α production. Thus, memory cells demonstrated no increase in TCR responsiveness to suboptimal ligands, confirming that naive and memory CD8 T cells have similar early TCR signaling. In addition, we found no evidence that memory cells have a widened responsiveness to a spectrum of related ligands.

We also investigated the possibility that CD3 phosphorylation could be sustained for different time frames in naive, effector, and

memory T cells. We stimulated cells for 2, 10, and 20 min (Fig. 2*D*), and for up to 20 h (Fig. 2*E*) with peptide-pulsed, washed APCs. Again, we found no difference in the phosphorylation of CD3ζ or ZAP-70 (data not shown) over time. We were able to measure inducible CD3ζ phosphorylation for an extended period of time (up to 5 h), somewhat longer than previously observed in cultured cell lines. However, this was true for all cells alike. Thus, signal initiation was not prolonged in memory T cells as might have been expected.

We next analyzed constitutive CD3ζ phosphorylation in samples containing only Ag-specific cells and no other T cells. We purified cells by FACS sorting with anti-CD8 and anti-Thy-1.1 Abs. This enabled us to obtain samples with 97% P14 cells. The constitutive phosphoform of CD3ζ, p21, was present to a similar degree in effector and memory T cells (Fig. 2*F*), while it seemed elevated in naive cells. The total CD3ζ protein content was also higher in naive P14 T cells (Fig. 2*F*). This correlated with higher TCR levels on naive P14 cells, as analyzed by FACS (data not shown). We had not noticed this difference previously (Fig. 2, *A–E*), because effector and memory samples were of lower purity and contained naive T cells of other specificities that would not respond in our assays. However, this difference did not make naive cells more sensitive to Ag stimulation (Fig. 2, *A–C*). Thus, we ruled out that memory CD8 T cells have elevated levels of phospho-CD3ζ, as might have been expected for cells with increased signaling capacity.

More phospho-ZAP-70 in effector cells

ZAP-70 kinase binds to phospho-CD3, is phosphorylated by *src* kinases, and then acts on downstream signaling molecules. It has been reported that the *src* kinase $p56^{lck}$ is up-regulated in memory CD8 T cells (20, 21), while another study found more CD8-bound $p56^{lck}$, but no difference in the $p56^{lck}$ amount (19). Increased $p56^{lck}$ could lead to enhanced phosphorylation of ZAP-70. We therefore also determined total phospho-ZAP-70 in activated naive, effector, and memory cells. We directly precipitated all ZAP-70, not just ZAP-70 associated with CD3ϵ. The amount of phospho-Zap-70 was similar in naive and memory cells, although in some experiments, it was slightly reduced in memory cells (Fig. 3*A*). In addition, we consistently found more phospho-ZAP-70 in effector cells, although ZAP-70 protein was similar (Fig. 3*B*, *upper band*). Thus, ZAP-70 is more effectively phosphorylated in effector cells.

We next examined the level of *src* family kinases in P14 T cells (Fig. 3*C*). Effector cells had more $p56^{lck}$ than memory and naive cells, as previously reported (21). Thus, increased phospho-ZAP-70 in effector cells could be due to elevated $p56^{lck}$. Memory cells only had slightly increased levels of $p56^{lck}$ when compared with naive cells. In addition, we analyzed the expression of another *src* kinase involved in T cell signal transduction, $p56^{fyn}$ (Fig. 3*C*). $P56^{fyn}$ was up-regulated in both memory and effector cells. Despite these changes, CD3 phosphorylation and ZAP-70 signal transduction were not up-regulated in memory CD8 cells. Thus, increased *src* family kinase expression might be inconsequential in memory cells, or might influence other signaling events.

More lipid rafts with more phosphoproteins in effector and memory cells

We next addressed whether signaling events further downstream of the TCR were augmented in memory cells. Lipid rafts are specialized signaling compartments in T cells. We therefore examined the size and phosphoprotein content of lipid rafts. We first assessed surface GM1 and asialo-GM1 levels. GM1 is a glycosphingolipid specifically enriched in lipid rafts. It has been used as a lipid raft marker and can be detected with the cholera toxin B subunit by

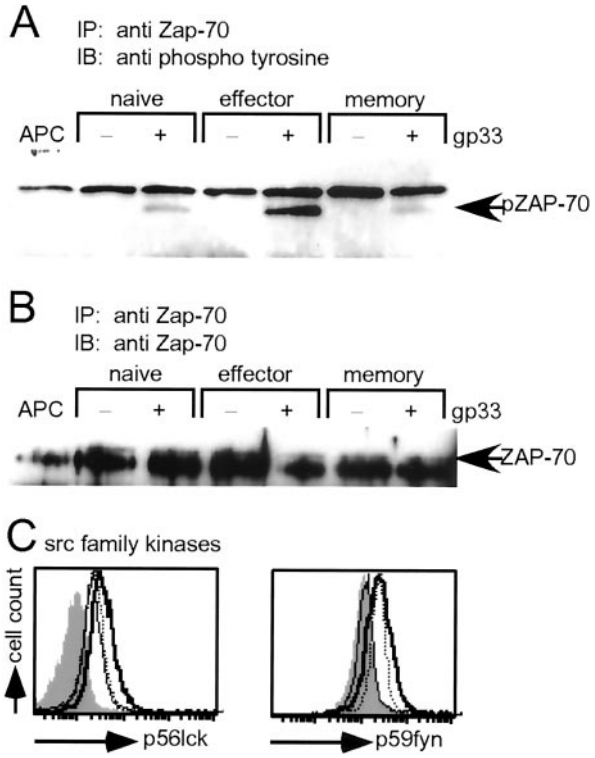

FIGURE 3. The activation of ZAP-70 is similar in naive and memory T cells, and increased in effector T cells. *A*, Antiphosphotyrosine immunoblot. A total of 10×10^6 purified P14 cells was stimulated for 10 min with APCs prepulsed with 10 μg of gp33. After lysis, Zap-70 was precipitated using rabbit anti-ZAP-70, and analyzed by antiphosphotyrosine immunoblotting. ZAP-70 was most phosphorylated in effector P14 cells. The experiment is representative of four independent experiments. *B*, Anti-ZAP-70 immunoblot. The immunoblot shown in *A* was stripped and reprobed with rabbit anti-ZAP-70. Similar levels of ZAP-70 protein were present in each lane. *C*, Levels of the *src* family kinase $p56^{lck}$ and $p56^{fyn}$ in naive, effector, and memory P14 cells (thin, bold, dotted line, respectively; filled line, isotype control). Cells were gated on $D^b gp33^+$, $CD8^+$, and analyzed by intracellular FACS using anti-$p56^{lck}$ FITC or anti-$p56^{fyn}$ FITC. The data were similar in three independent experiments. Isotype controls were performed with anti-IgG2b FITC and polyclonal goat FITC serum.

flow cytometry. Surface GM1 levels were higher in both effector and memory T cells when compared with naive cells (Fig. 4*A*). Thus, lipid rafts of memory CD8 T cells are more extensive. We also examined the amount of asialo-GM1 (aGM1), an altered GM1 form that is stripped of its sialic acid moieties and therefore of its negative surface charges. Such aGM1 forms are present on NK cells, and also on activated T cells (34). We found that aGM1 was highly expressed on the surface of memory T cells, to a lesser degree on effector, and the least on naive cells (Fig. 4*A*). Thus, lipid rafts of memory T cells are not only more extensive, but also contain qualitatively different glycolipids. Because aGM1 lacks the negatively charged sialic acid, it might allow for the formation of tighter lipid raft clusters (35, 36).

We next determined the phosphoprotein content of lipid rafts. We fractionated cell lysates into lipid raft and soluble fractions using sucrose gradient centrifugation. Because such experiments require large cell numbers, we were only able to analyze unstimulated cells. We incubated mechanically disrupted cells in 1% Brij 58, a detergent that leaves lipid rafts insoluble (29). We collected 12 fractions after sucrose gradient centrifugation. We confirmed that fractions 1–4 contained lipid raft-associated proteins by assessing $p56^{lck}$ content. $p56^{lck}$ partitions mainly to soluble fractions

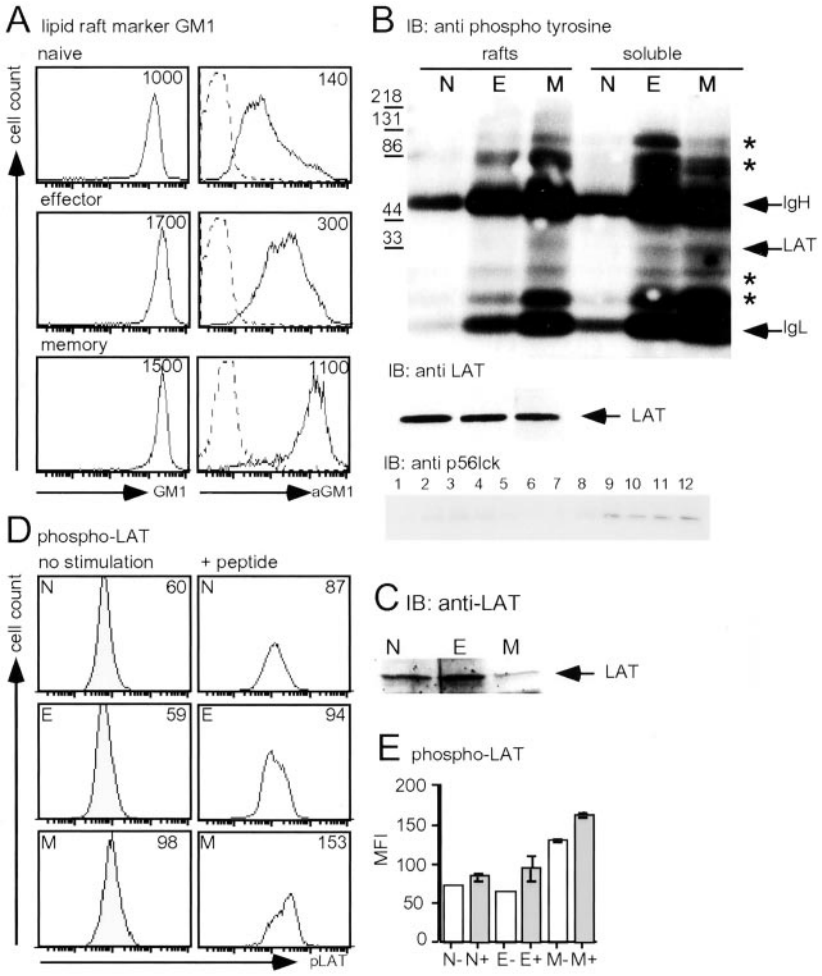

FIGURE 4. Increased lipid rafts, phosphotyrosine content, and phospho-LAT in memory T cells. *A*, Lipid raft markers GM1 and aGM1 were visualized by FACS using cholera toxin B subunit or rabbit anti-aGM1. Cells are gated on $D^b gp33^+$. The dotted line represents control staining with rabbit serum. *B*, Antiphosphotyrosine analysis of membrane compartments. A total of 20×10^6 purified P14 cells was mechanically disrupted and incubated in 1% Brj 58, followed by sucrose gradient centrifugation. Twelve fractions were harvested from the top, and analyzed by immunoblotting for $p56^{lck}$ (*bottom panel*). Fractions 1–4 were pooled (rafts, insoluble in 1% Brj 58), as were 8–11 (soluble). Proteins were concentrated and analyzed by antiphosphotyrosine immunoblotting. Unidentified proteins are marked with ∗. Molecular masses (in kDa) and the position of Ig (anti-Thy-1.1, IgH, and IgL) are indicated. More anti-Thy-1.1 Ab bound to effector and memory cells, because they have higher Thy-1.1 surface levels. The blot was stripped and reprobed with anti-LAT (*middle panel*). The experiment was performed four times. *C*, Immunoblot for LAT in FACS-sorted naive, effector, and memory P14 cells. LAT levels are not increased in memory cells. *D* and *E*, Induction of phospho-LAT (pY191). Mice were injected with 100 μg gp33 to activate P14 cells. Fifteen minutes later, splenocytes were fixed and stained with anti-phospho-LAT (Y191) or control rabbit serum (data not shown), followed by goat anti-rabbit FITC. Shown is FACS analysis of TCR-Vα2-gated (N) or Thy-1.1-gated cells (E, M) from unstimulated (*left*) or stimulated mice (*right*). The numbers indicate mean fluorescence intensities (MFIs). The MFIs for control rabbit serum were 7, 10, and 9 for N, E, and M, respectively (data not shown). In *E*, average MFIs of two unstimulated and four stimulated mice of the same experiment are given. Error bars represent the SEM. The experiment was performed three times with at least five mice per group.

but a small portion localizes to lipid rafts, and this can be used to identify lipid rafts with great sensitivity. (Fig. 4*B*, *bottom panel*). We pooled lipid raft (1–4) or soluble fractions (8–11), and concentrated them because phosphoproteins were too diluted for direct analysis. We found several important differences between naive, effector, and memory T cells (Fig. 4*B*). Most strikingly, more phosphoproteins were consistently present in lipid rafts of both effector and memory T cells. We repeated the experiment after purification with anti-CD8 magnetic beads to rule out that the observed differences were due to anti-Thy-1.1 stimulation, and obtained similar results (data not shown). Thus, increased phosphoproteins in lipid rafts suggests that Ag-experienced cells have more signaling molecules, more tyrosine kinase activity, or less inhibitory phosphatase activity associated with lipid rafts. All of these scenarios are likely to increase signal transduction capacity.

One of the phosphoproteins is likely to be LAT. It comigrated with anti-LAT precipitates as an internal size indicator (data not shown). We also performed immunoblotting to identify LAT. Anti-LAT recognized a single band of 36 kDa when the experiment was reblotted (Fig. 4*B*). This protein was present in lipid rafts of naive, effector, and memory T cells to a similar degree (Fig. 4*B*). The identity of the other phosphoproteins in Fig. 4*B* remained unclear (see proteins marked with ∗). We could not identify ZAP-70, $p56^{lck}$, $p56^{fyn}$, phospholipase Cγ, Vav, Grb-2, and phosphatidylinositol-3 kinase by immunoblotting because of low sensitivity (data not shown). To further confirm that all cell types expressed LAT, we also analyzed LAT in unfractionated samples of higher purity (Fig. 4*C*).

We next analyzed LAT phosphorylation after specific activation of P14 cells in vivo. We injected gp33 peptide i.v. into live naive P14 mice, or into P14 effector or memory mice. We sacrificed them 15 min later, and immediately fixed splenocytes to preserve activated molecules (37). We then analyzed phospho-LAT by intracellular FACS analysis using an Ab to phospho-LAT (tyrosine 191). This distal tyrosine is specifically phosphorylated after activation, and facilitates binding of Grb2 and Gads (38). Memory P14 cells had the highest presence of phospho-LAT before stimulation with gp33, corresponding to the increase in phospho-LAT in lipid rafts of freshly isolated memory cells (Fig. 4*D*, *left panel*). Memory P14 T cells also induced phospho-LAT to the highest degree upon activation, as evident by the largest mean fluorescence intensity (see Fig. 4*D* for one representative mouse, and 4*E* for an average of multiple mice). Thus, this further demonstrated that memory cells induce phosphorylation of the linker LAT most efficiently. Phospho-LAT is required for the assembly of higher order signaling complexes in lipid rafts. The increased presence of phospho-LAT in lipid rafts therefore strongly indicates increased signal transduction at this checkpoint in memory CD8 T cells.

MAP kinase signaling pathways are up-regulated in memory CD8 T cells

The signaling complexes assembled by phospho-LAT have multiple components. One important group of effector signaling molecules are members of the MAP kinase family. This extensive family includes the ERKs, JNKs, p38 MAP kinases, as well as MKKs (39). Next, we determined the activation status of members of the MAP kinase family. For these experiments, we again stimulated P14 T cells in vivo, followed by immediate fixation of splenocytes to preserve active enzyme states. We then performed

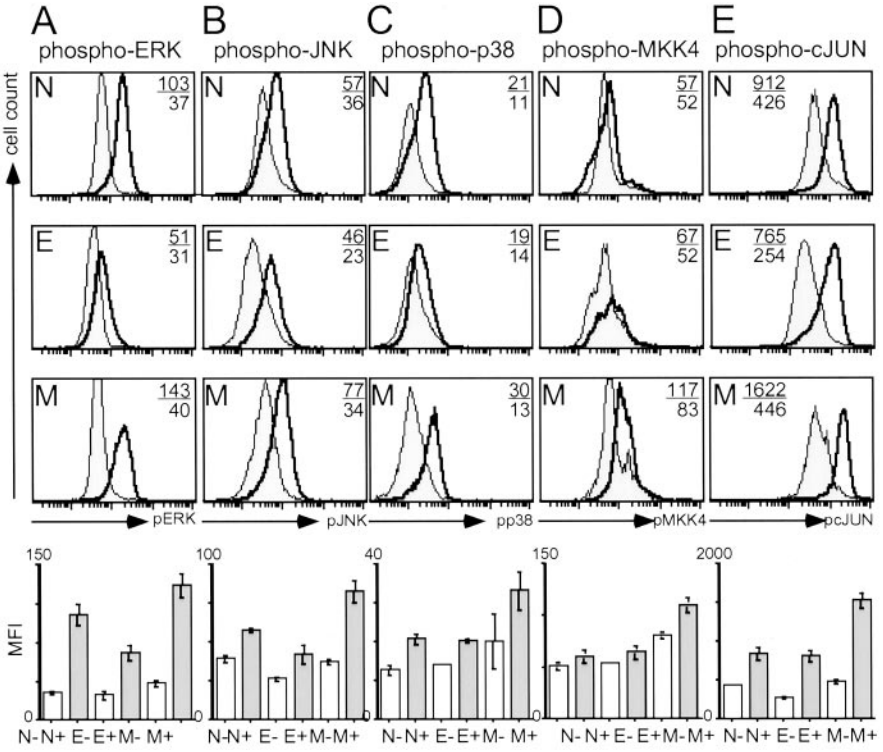

FIGURE 5. MAP kinase signaling pathways are up-regulated in memory CD8 T cells. *A–E*, P14 cells were activated for 15 min in vivo after i.v. injection of 100 μg gp33. Splenocytes were immediately fixed and stained with rabbit anti-phospho-ERK (*A*), phospho-JNK (*B*), phospho-p38 kinase (*C*), phospho-MKK4 (*D*), as well as rabbit control serum (data not shown) and anti-rabbit FITC. Staining with mouse anti-phospho-c-Jun (*E*) was done after FcR blockade and followed by anti-mouse IgG1 FITC. Naive cells (N) are gated on TCR-Vα2$^+$, effector (E), and memory (M) on Thy-1.1$^+$ cells. The gray filled histograms represent data from one unstimulated mouse; the thick line represents data from one stimulated mouse. Numbers indicate mean fluorescence intensities (MFIs) of unstimulated (*lower*) or stimulated (*upper*) cells. The *bottom panels* give averages of two unstimulated, and three to four stimulated mice from the same experiment. Error bars represent SEM. Results are representative of four independent experiments of groups of at least four mice (*A–D*), or of two such experiments (*E*).

intracellular staining using phospho-specific reagents. Phospho ERK-1/2 (p42/p44) was most vigorously induced in memory P14 cells (Fig. 5*A*). It was also consistently higher in memory cells before peptide stimulation when compared with naive cells, although these differences were slight. The difference between activated naive and memory cells was also striking for active JNK, as measured with an Ab to the dually phosphorylated Thr/Pro/Tyr region of JNK2, as well as for phospho-p38 (Ab to phospho-Thr^{180}/Tyr^{182}; Fig. 5, *B* and *C*). Effector cells showed a marked defect in the inducible phosphorylation of ERK and JNK, and behaved similarly to naive cells with regard to pp38. We also examined MKK4 as a representative of an upstream kinase that acts on JNK and p38. Consistent with increased JNK and p38 phosphorylation, phospho-MKK4 was also highest in memory CD8 T cells (Fig. 5*D*). In addition, we noticed that a portion of unstimulated memory CD8 T cells constitutively had phospho-MKK4 in all experiments. This indicates that the MAP kinase pathway is constitutively used in a portion of memory cells in vivo. Finally, we analyzed the phosphorylation of c-JUN, a transcription factor that is phosphorylated by JNK. Again, c-JUN phosphorylation was most impressively induced in memory P14 cells (Fig. 5*E*). Thus, we conclude that increased MAP kinase signaling was transduced to the level of transcriptional regulation in memory CD8 T cells. In summary, we found that memory CD8 T cells have increased ability to engage multiple downstream MAP kinase signaling pathways.

Memory CD8 T cells exist in two related subsets: T_{CM} cells persist for longer periods of time, have higher proliferative potential, are CD62L^{high}, CCR7^{high} and provide more protective immunity against reinfection than T_{EM} cells (CD62L^{low}, CCR7^{low}) (32). We next addressed whether T_{CM} cells also have higher signaling capacity than T_{EM} cells. T_{CM} P14 cells had higher levels of GM1 (Fig. 6*A*). Thus, the lipid raft compartment is larger on the surface of this memory subset. We next quantitatively examined the induction of signaling intermediates. CD62L is shed from the surface after T cell activation. We therefore first separated P14 memory CD62L$^{high/low}$ cells with anti-CD62L-coated magnetic beads and subsequently stimulated them with Ag in vitro. The levels of pLAT and pERK were reproducibly higher in unstimulated T_{CM} cells (Fig. 6, *B* and *C*). Upon activation, phosphorylation of both LAT and ERK proceeded to a higher level than in T_{EM} cells (Fig. 6, *B*

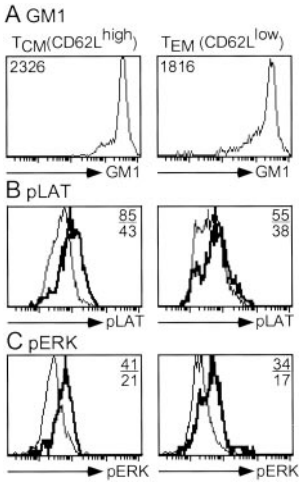

FIGURE 6. Signaling capacity of T_{CM} and T_{EM} memory subsets. *A*, Surface GM1 levels as an indicator of lipid raft size in CD62L^{high} (T_{CM}) and CD62L^{low} (T_{EM}) P14 cells. Cells were stained with D^{b}gp33 tetramer, anti-CD62L, and cholera toxin B and analyzed by FACS. Numbers indicate mean fluorescence intensities. *B* and *C*, T_{CM} cells have higher LAT and ERK signaling capacity than T_{EM} cells. P14 memory cells were separated into CD62L$^{high/low}$ subsets with anti-CD62L magnetic beads and stimulated with Ag in vitro for 30 min. Cells were fixed and stained with rabbit anti-phospho-LAT and anti-phospho-ERK. Cells were gated on Thy-1.1$^+$ cells. The gray filled histograms represent unstimulated cells; the bold lines stimulated cells. Numbers indicate mean fluorescence intensities (MFIs) of unstimulated (*lower number*) or stimulated (*upper number*) cells. Results are representative of three independent experiments.

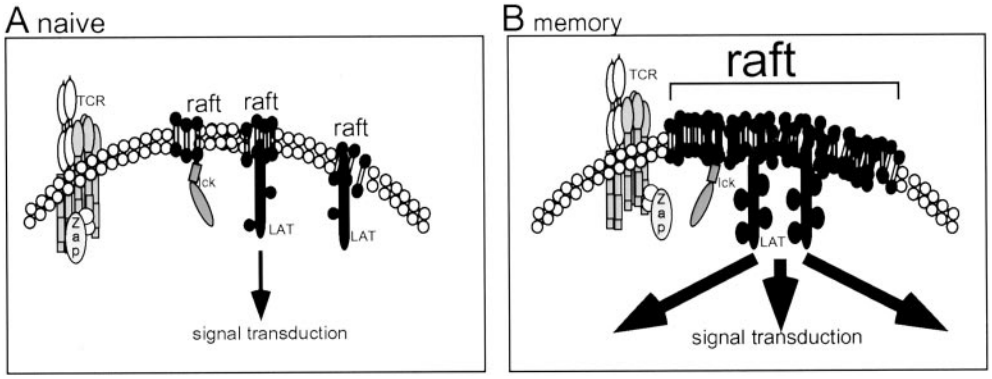

FIGURE 7. Model: Memory CD8 T cells have an up-regulated signaling machinery in the lipid raft signaling compartment. *A*, In naive cells, lipid rafts are not extensive, and do not contain signaling proteins in close proximity. *B*, In memory T cells, lipid rafts are more extensive and contain more phosphosignaling proteins such as phospho-LAT before TCR engagement. Upon activation, memory T cells might assemble signaling complexes within close proximity and process signals more effectively in lipid rafts. Further downstream, several MAP kinase signaling pathways are up-regulated. Increasing the signaling capacity of lipid rafts rather than at the TCR itself could be a powerful way to increase the effectiveness of signaling without increasing the responsiveness to Ag. We propose that this is a mechanism that can avoid cross-reactivity and autoimmunity of the TCR while at the same time augmenting signal transduction.

and *C*). We conclude that T_{CM} cells have increased signaling capacity over T_{EM} cells, correlating with their increased responsiveness to Ag upon secondary infection. We recently proposed that naive cells differentiate in a linear manner from naive, to effector, to T_{EM}, and finally T_{CM} cells (32). We now find that this differentiation process is accompanied by a biochemical change in the lipid raft compartment and an increase in signaling capacity.

Discussion

In this study, we examine proximal TCR signal transduction and lipid rafts of Ag-specific memory and naive CD8 T cells. We find that the initial phosphorylation of the CD3 complex is similar in naive and memory T cells. Thus, the TCR in naive T cells is equally sensitive as in memory T cells. However, memory T cells have more extensive lipid rafts. Lipid rafts in memory T cells contain more phosphosignaling proteins before TCR engagement (schematically shown in Fig. 7). This higher concentration of signaling complexes within close proximity might make memory cells superior in phosphorylating critical signaling molecules upon cellular activation, as we have observed for LAT and MAP kinases. Memory T cells thus seem to process intracellular signals more effectively downstream of the TCR. Increasing the signaling capacity of lipid rafts rather than of the TCR itself could therefore be a powerful way to increase the effectiveness of signaling without increasing the responsiveness to Ag. We thus propose that this could be a mechanism that allows memory T cells to avoid cross-reactivity and autoimmunity at the TCR while at the same time augmenting signal transduction.

This work describes previously unrecognized molecular changes in memory CD8 T cells. It will be important to test the significance of such signaling alterations once it is technically possible to genetically manipulate memory T cells.

Our data demonstrate that memory CD8 T have higher constitutive tyrosine phosphorylation at several signaling checkpoints downstream of the TCR. It is important to point out that the cells have not been restimulated recently, because Ag is cleaned within a week of LCMV (Armstrong) infection (6, 7). Consistent with this, cells show no recent activation markers (they are $CD69^{low}$, $CD25^{low}$, and small in size; data not shown). The constitutive intracellular activation state might be due to changes in gene expression of signaling molecules (21). In addition, permanent reconfiguration of the plasma membrane and cytoskeleton might allow closer contact of signaling complexes even in the absence of stimulation in memory cells.

Recent data suggest that T cells regulate the extent and composition of the lipid raft signaling compartment throughout T cell development. Indeed, Th1 and Th2 cells differ in their dependence on lipid raft structures for signal transduction and differentially partition TCRζ and CD45 to lipid rafts in response to antigenic stimulation (40).

We found no differences in TCR signal initiation at the CD3 complex despite a more extensive lipid raft compartment in memory T cells. We therefore conclude that the extent of pre-existing lipid rafts is not limiting for the very first phosphorylation steps of signal initiation at the TCR. This is consistent with recent findings that initial TCR signaling precedes immunological synapse formation (41).

It has previously been reported that activated T cells undergo activation-induced membrane changes, and that this leads to an up to 20-fold increase in TCR avidity for soluble dimeric MHC class I molecules (22). As a consequence, the authors suggested that activated cells can better sense low-density Ag in peripheral tissues. We did not find greater responsiveness when we measured the intracellular signaling output of the TCR on Ag-experienced cells. However, effector T cells contained less TCR on their surface (data not shown), most likely due to activation-induced TCR down-regulation. Thus, TCR sensitivity might be determined by low TCR number and increased TCR avidity on effector cells.

Our analysis included effector CD8 T cells. Although infectious virus has been cleared 7 days after LCMV infection, we cannot exclude that some of the cells are stimulated by persisting Ag on dendritic cells at this time point. Effector cells had more inducible phospho-ZAP-70 than both naive and memory CD8 T cells. Effector cells thus had up-regulated early signal transduction, as previously observed (42). We also observed that effector cells had more phosphoproteins in lipid rafts than naive T cells, but less than memory cells. However, effector cells showed a marked defect in their ability to phosphorylate ERK-1/2. Thus, increased early signals seemed to be abrogated by a down-regulation of more distal signaling. This down-regulation of later signaling events is in marked contrast to CD4 effector cells (18). The down-regulation might serve to specifically limit the proliferative ability of effector CD8 T cells (21).

Naive, effector, and memory T cells are differently dependent on costimulation (43, 44). Previous studies have suggested that costimulators function to direct migration of lipid rafts to the site of TCR contact (15, 45, 46). It is therefore feasible that lipid raft signaling is differently regulated by costimulation in memory cells. Experiments are underway to address the role of costimulation in signaling events in memory cells.

We were surprised at first to not find differences in CD3 phosphorylation between naive and memory T cells. CD3ζ phosphorylation proceeds in discreet steps, and these can be driven by the binding of suboptimal ligands to the TCR (28). It is tempting to speculate that increasing phospho-CD3ζ might bear the inherent risk of cross-reactivity to different TCR ligands. Cross-reactivity to other ligands might be particularly dangerous for memory T cells because of potential autoimmunity. These long-lived cells with increased effector functions and recirculation patterns have ample opportunity to attack self in peripheral tissues. We believe that sensing low-density ligands more effectively is not desirable for memory T cells in the periphery. Rather, by differentiating the lipid raft compartment, memory T cells seem to use a mechanism to increase the effectiveness of signal transduction without altering the sensitivity of the TCR.

Acknowledgments

We thank Larry Samelson for rabbit anti-LAT and advice. We thank Weiguo Zhang and Linda Baum for advice, Paul Allen for rabbit anti-CD3ζ, Gil Kersh for critical reading of the manuscript, and Patryce Yeiser and Bogna Konieczny for excellent technical assistance.

References

1. Kaech, S. M., E. J. Wherry, and R. Ahmed. 2002. Effector and memory T-cell differentiation: implications for vaccine development. *Nat. Rev. Immunol. 2:251.*
2. Dutton, R. W., L. M. Bradley, and S. L. Swain. 1998. T cell memory. *Annu. Rev. Immunol. 16:201.*
3. Sprent, J., and C. D. Surh. 2002. T cell memory. *Annu. Rev. Immunol. 20:551.*
4. Murali-Krishna, K., and R. Ahmed. 2000. Cutting edge: naive T cells masquerading as memory cells. *J. Immunol. 165:1733.*
5. Pircher, H., K. Burki, R. Lang, H. Hengartner, and R. M. Zinkernagel. 1989. Tolerance induction in double specific T-cell receptor transgenic mice varies with antigen. *Nature 342:559.*
6. Lau, L. L., B. D. Jamieson, T. Somasundaram, and R. Ahmed. 1994. Cytotoxic T-cell memory without antigen. *Nature 369:648.*
7. Murali-Krishna, K., L. L. Lau, S. Sambhara, F. Lemonnier, J. Altman, and R. Ahmed. 1999. Persistence of memory CD8 T cells in MHC class I-deficient mice. *Science 286:1377.*
8. Kane, L. P., J. Lin, and A. Weiss. 2000. Signal transduction by the TCR for antigen. *Curr. Opin. Immunol. 12:242.*
9. Van Leeuwen, J. E., and L. E. Samelson. 1999. T cell antigen-receptor signal transduction. *Curr. Opin. Immunol. 11:242.*
10. Gil, D., W. W. Schamel, M. Montoya, F. Sanchez-Madrid, and B. Alarcon. 2002. Recruitment of Nck by CD3 ϵ reveals a ligand-induced conformational change essential for T cell receptor signaling and synapse formation. *Cell 109:901.*
11. Zhang, W., R. P. Trible, and L. E. Samelson. 1998. LAT palmitoylation: its essential role in membrane microdomain targeting and tyrosine phosphorylation during T cell activation. *Immunity 9:239.*
12. Zhang, W., J. Sloan-Lancaster, J. Kitchen, R. P. Trible, and L. E. Samelson. 1998. LAT: the ZAP-70 tyrosine kinase substrate that links T cell receptor to cellular activation. *Cell 92:83.*
13. Simons, K., and E. Ikonen. 1997. Functional rafts in cell membranes. *Nature 387:569.*
14. Janes, P. W., S. C. Ley, A. I. Magee, and P. S. Kabouridis. 2000. The role of lipid rafts in T cell antigen receptor (TCR) signalling. *Semin. Immunol. 12:23.*
15. Miceli, M. C., M. Moran, C. D. Chung, V. P. Patel, T. Low, and W. Zinnanti. 2001. Co-stimulation and counter-stimulation: lipid raft clustering controls TCR signaling and functional outcomes. *Semin. Immunol. 13:115.*
16. Farber, D. L., M. Luqman, O. Acuto, and K. Bottomly. 1995. Control of memory CD4 T cell activation: MHC class II molecules on APCs and CD4 ligation inhibit memory but not naive CD4 T cells. *Immunity 2:249.*
17. Farber, D. L., O. Acuto, and K. Bottomly. 1997. Differential T cell receptor-mediated signaling in naive and memory CD4 T cells. *Eur. J. Immunol. 27:2094.*
18. Hussain, S. F., C. F. Anderson, and D. L. Farber. 2002. Differential SLP-76 expression and TCR-mediated signaling in effector and memory CD4 T cells. *J. Immunol. 168:1557.*
19. Bachmann, M. F., A. Gallimore, S. Linkert, V. Cerundolo, A. Lanzavecchia, M. Kopf, and A. Viola. 1999. Developmental regulation of Lck targeting to the CD8 coreceptor controls signaling in naive and memory T cells. *J. Exp. Med. 189:1521.*
20. Slifka, M. K., and J. L. Whitton. 2001. Functional avidity maturation of $CD8^+$ T cells without selection of higher affinity TCR. *Nat. Immun. 2:711.*
21. Kaech, S. M., S. Hemby, E. Kersh, and R. Ahmed. 2002. Molecular and functional profiling of memory CD8 T cell differentiation. *Cell 111:837.*
22. Fahmy, T. M., J. G. Bieler, M. Edidin, and J. P. Schneck. 2001. Increased TCR avidity after T cell activation: a mechanism for sensing low-density antigen. *Immunity 14:135.*
23. Tuosto, L., I. Parolini, S. Schroder, M. Sargiacomo, A. Lanzavecchia, and A. Viola. 2001. Organization of plasma membrane functional rafts upon T cell activation. *Eur. J. Immunol. 31:345.*
24. Mombaerts, P., A. R. Clarke, M. A. Rudnicki, J. Iacomini, S. Itohara, J. J. Lafaille, L. Wang, Y. Ichikawa, R. Jaenisch, M. L. Hooper, et al. 1992. Mutations in T-cell antigen receptor genes α and β block thymocyte development at different stages. *Nature 360:225.*
25. Zimmerman, C., K. Brduscha-Riem, C. Blaser, R. M. Zinkernagel, and H. Pircher. 1996. Visualization, characterization, and turnover of $CD8^+$ memory T cells in virus-infected hosts. *J. Exp. Med. 183:1367.*
26. Ahmed, R., A. Salmi, L. D. Butler, J. M. Chiller, and M. B. Oldstone. 1984. Selection of genetic variants of lymphocytic choriomeningitis virus in spleens of persistently infected mice: role in suppression of cytotoxic T lymphocyte response and viral persistence. *J. Exp. Med. 160:521.*
27. Bachmann, M. F., D. E. Speiser, A. Zakarian, and P. S. Ohashi. 1998. Inhibition of TCR triggering by a spectrum of altered peptide ligands suggests the mechanism for TCR antagonism. *Eur. J. Immunol. 28:3110.*
28. Kersh, E. N., A. S. Shaw, and P. M. Allen. 1998. Fidelity of T cell activation through multistep T cell receptor ζ phosphorylation. *Science 281:572.*
29. Montixi, C., C. Langlet, A. M. Bernard, J. Thimonier, C. Dubois, M. A. Wurbel, J. P. Chauvin, M. Pierres, and H. T. He. 1998. Engagement of T cell receptor triggers its recruitment to low-density detergent-insoluble membrane domains. *EMBO J. 17:5334.*
30. Wessel, D., and U. I. Flugge. 1984. A method for the quantitative recovery of protein in dilute solution in the presence of detergents and lipids. *Anal. Biochem. 138:141.*
31. Murali-Krishna, K., J. D. Altman, M. Suresh, D. J. Sourdive, A. J. Zajac, J. D. Miller, J. Slansky, and R. Ahmed. 1998. Counting antigen-specific CD8 T cells: a reevaluation of bystander activation during viral infection. *Immunity 8:177.*
32. Wherry, E. J., V. Teichgräber, T. Becker, D. Masopust, S. M. Kaech, R. Antia, U. H. von Andrian, and R. Ahmed. 2003. Lineage relationship and protective immunity of memory CD8 T cell subsets. *Nat. Immun. 4:225.*
33. Evavold, B. D., J. Sloan-Lancaster, and P. M. Allen. 1993. Tickling the TCR: selective T-cell functions stimulated by altered peptide ligands. *Immunol. Today 14:602.*
34. Slifka, M. K., R. R. Pagarigan, and J. L. Whitton. 2000. NK markers are expressed on a high percentage of virus-specific $CD8^+$ and $CD4^+$ T cells. *J. Immunol. 164:2009.*
35. Xu, Z., and A. Weiss. 2002. Negative regulation of CD45 by differential homodimerization of the alternatively spliced isoforms. *Nat. Immun. 3:764.*
36. Daniels, M. A., K. A. Hogquist, and S. C. Jameson. 2002. Sweet 'n' sour: the impact of differential glycosylation on T cell responses. *Nat. Immun. 3:903.*
37. Zell, T., A. Khoruts, E. Ingulli, J. L. Bonnevier, D. L. Mueller, and M. K. Jenkins. 2001. Single-cell analysis of signal transduction in CD4 T cells stimulated by antigen in vivo. *Proc. Natl. Acad. Sci. USA 98:10805.*
38. Zhang, W., R. P. Trible, M. Zhu, S. K. Liu, C. J. McGlade, and L. E. Samelson. 2000. Association of Grb2, Gads, and phospholipase C-γ1 with phosphorylated LAT tyrosine residues: effect of LAT tyrosine mutations on T cell antigen receptor-mediated signaling. *J. Biol. Chem. 275:23355.*
39. Rincon, M. 2001. MAP-kinase signaling pathways in T cells. *Curr. Opin. Immunol. 13:339.*
40. Balamuth, F., D. Leitenberg, J. Unternaehrer, I. Mellman, and K. Bottomly. 2001. Distinct patterns of membrane microdomain partitioning in Th1 and Th2 cells. *Immunity 15:729.*
41. Lee, K. H., A. D. Holdorf, M. L. Dustin, A. C. Chan, P. M. Allen, and A. S. Shaw. 2002. T cell receptor signaling precedes immunological synapse formation. *Science 295:1539.*
42. Ahmadzadeh, M., S. F. Hussain, and D. L. Farber. 1999. Effector CD4 T cells are biochemically distinct from the memory subset: evidence for long-term persistence of effectors in vivo. *J. Immunol. 163:3053.*
43. Pihlgren, M., P. M. Dubois, M. Tomkowiak, T. Sjogren, and J. Marvel. 1996. Resting memory $CD8^+$ T cells are hyperreactive to antigenic challenge in vitro. *J. Exp. Med. 184:2141.*
44. Dubey, C., M. Croft, and S. L. Swain. 1996. Naive and effector CD4 T cells differ in their requirements for T cell receptor versus costimulatory signals. *J. Immunol. 157:3280.*
45. Viola, A., S. Schroeder, Y. Sakakibara, and A. Lanzavecchia. 1999. T lymphocyte costimulation mediated by reorganization of membrane microdomains. *Science 283:680.*
46. Patel, V. P., M. Moran, T. A. Low, and M. C. Miceli. 2001. A molecular framework for two-step T cell signaling: Lck Src homology 3 mutations discriminate distinctly regulated lipid raft reorganization events. *J. Immunol. 166:754.*